THE ASTROPHYSICAL JOURNAL, 225:40–55, 1978 October 1

H I, GALAXY COUNTS, AND REDDENING: VARIATION IN THE GAS-TO-DUST RATIO, THE EXTINCTION AT HIGH GALACTIC LATITUDES, AND A NEW METHOD FOR DETERMINING GALACTIC REDDENING*

DAVID BURSTEIN
Board of Studies, Astronomy and Astrophysics, University of California, Santa Cruz

AND

CARL HEILES
Astronomy Department, University of California, Berkeley
Received 1978 March 3; accepted 1978 April 5

ABSTRACT

We reanalyze the interrelationships among Shane-Wirtanen galaxy counts, H I column densities, and reddenings, and resolve many of the problems raised by Heiles. These problems were caused by two factors: subtle biases in the reddening data and a variable gas-to-dust ratio in the galaxy. We present a compilation of reddenings for RR Lyrae stars and globular clusters which are on the same system and which we believe to be relatively free of biases. The extinction at the galactic poles, as determined by galaxy counts, is reexamined by using a new method to analyze galaxy counts. This new method partially accounts for the nonrandom clustering of galaxies and permits a reasonable estimate of the error in log $N_{\rm gal}$ as a function of latitude. The analysis shows that galaxy counts (or galaxy cluster counts) are too noisy to allow direct determination of the extinction, or variation in extinction, near the galactic poles. From all available data, we conclude that the reddening at the poles is small [≤ 0.02 mag in $E(B-V)$ over much of the north galactic pole] and irregularly distributed. We find that there are zero offsets in the relations between $E(B-V)$ and H I, and between galaxy counts and H I, which are at least partly the result of an instrumental effect in the radio data. We also show that the gas-to-dust ratio can vary by a factor of 2 from the average, and we present two methods for correcting for this variability in predicting the reddening of objects which are located outside of the galactic absorbing layer. We present a prescription for predicting these reddenings; in the area of sky covered by the Shane-Wirtanen galaxy counts, the error in these predictions is, on average, less than 0.03 mag in $E(B-V)$.

Subject headings: galaxies: clusters of — interstellar: matter — radio sources: 21 cm radiation

I. INTRODUCTION

Despite many attempts to find a reliable method to measure the reddening of extragalactic objects, a generally accepted "best" method has not yet been established. As shown in Paper I (Burstein and Heiles 1978), smooth csc $|b|$ models do not work well because of the patchiness of the interstellar dust. Ways to account for the irregularities in the reddening distribution have centered on measuring either the variations in galaxy counts (e.g., Shane and Wirtanen 1967) or the H I column density (e.g., Knapp and Kerr 1974), and then deriving a relationship between these extinction indicators and the reddening. The previous large-scale investigation into the interdependence among H I, galaxy counts, and reddening (Heiles 1976) concluded that there were no simple relationships among these extinction indicators and produced some unresolved problems.

In this paper we further investigate the relationship among these quantities and are able to resolve many of the problems. Most of them originated because the gas-to-dust ratio is variable, a phenomenon which has previously been found by Seki (1973) in his study of the correlation between H I and galaxy counts and by UV observers in their studies of the interstellar medium (Jenkins and Savage 1974; Bohlin 1975; Savage *et al.* 1977). Comparison of the galaxy counts with H I column densities enables us to correct for the variable gas-to-dust ratio and to predict the value of $E(B-V)$ with considerable accuracy.

* *Lick Observatory Bulletin*, No. 807.

II. THE DATA

Table 1 lists the galaxy counts ($N_{\rm gal}$) and the neutral hydrogen column densities ($N_{\rm H}$) in the directions of 49 globular clusters, 84 RR Lyrae stars, and two early-type stars from Abt and Golson (1962). All of these objects have $|b| > 10°$ and z distances larger than 300 pc. The galaxy counts are derived from the numbers given by Shane and Wirtanen (1967, hereafter SW), corrected as in Heiles's (1976) work. The units are number per deg^2, averaged over 13 deg^2 centered on each object; $N_{\rm gal}$ is unavailable for objects with $\delta < -23°$ because of the southern limit of the SW

TABLE 1

REDDENING DATA FOR GLOBULAR CLUSTERS, RR LYRAE STARS, AND ABT AND GOLSON STARS: $|b| > 10°$

Object	l^{II}	b^{II}	$E(B-V)$	Source	N_H	log N_{gal}	R
			Globular Clusters—Southern				
NGC 104.......	305.9	−44.9	+0.04	1	246	...	...
NGC 362.......	301.6	−46.3	+0.02	1, 2	194	...	...
NGC 1261......	270.6	−52.1	0.00	1	114	...	...
NGC 2298......	245.6	−16.0	+0.08	1	441	...	...
NGC 2808......	282.2	−11.3	+0.25	2, 3	502	...	...
NGC 5139......	309.1	+15.1	+0.11	1	425	...	...
NGC 5286......	311.6	+10.6	+0.28	4	680	...	...
NGC 5824......	332.6	+22.1	+0.14	5	432	...	...
NGC 5986......	337.0	+13.3	+0.17	4	638	...	...
NGC 6397......	338.2	−12.0	+0.18	1	581	...	...
NGC 6541......	349.3	−11.2	+0.18	1	461	...	...
NGC 6584......	342.1	−16.4	+0.10	5	324	...	...
NGC 6637......	1.7	−10.3	+0.20	1	499	...	...
NGC 6652......	1.5	−11.4	+0.10	5	421	...	...
NGC 6715......	5.6	−14.1	+0.17	3	434	...	...
NGC 6723......	0.0	−17.3	+0.03	1, 6	292	...	...
NGC 6752......	336.5	−25.6	+0.04	1	226	...	...
NGC 6809......	8.8	−23.3	+0.03	3	389	...	...
			Globular Clusters—Northern				
NGC 288.......	149.7	−89.4	+0.03	7, 8	123	...	...
NGC 1904......	227.2	−29.3	+0.02	9	153	1.418	0.0
NGC 2419......	180.4	+25.3	+0.03	10	300	...	...
NGC 4147......	252.8	+77.2	+0.02	1	140	1.757	+0.5
NGC 4590......	299.6	+36.0	+0.03	3	331	...	...
NGC 5024......	333.0	+79.8	0.00	1	148	1.663	0.0
NGC 5053......	335.6	+78.9	+0.03	11	117	1.664	0.0
NGC 5272......	42.2	+78.7	+0.01	1	46.2	1.878	+1.0
NGC 5466......	42.1	+73.6	0.00	1	94	1.865	0.0
NGC 5634......	342.2	+49.3	+0.03	5	188	1.447	−1.0
NGC 5694......	331.1	+30.4	+0.09	5	394	...	...
NGC 5897......	342.9	+30.3	+0.11	1	458	1.179	0.0
NGC 5904......	3.9	+46.8	+0.03	1	192	1.760	+1.7
NGC 6093......	352.7	+19.4	+0.17	1, 12	570	0.740	−2.0
NGC 6171......	3.4	+23.0	+0.30	1	745	0.700	−2.0
NGC 6205......	59.0	+40.9	+0.02	1	104	1.542	0.0
NGC 6218......	15.7	+26.3	+0.17	1	409	1.152	−1.0
NGC 6229......	73.6	+40.3	+0.02	5, 13	96	1.568	0.0
NGC 6254......	15.1	+23.1	+0.27	1, 4	536	0.826	−3.0
NGC 6287......	0.1	+11.0	+0.40	5	798	0.342	0.0
NGC 6333......	5.5	+10.7	+0.37	5	849	0.204	0.0
NGC 6341......	68.4	+34.9	+0.02	1	144	1.657	+1.0
NGC 6356......	6.7	+10.2	+0.40	1, 5	904	0.114	0.0
NGC 6402......	21.3	+14.8	+0.37	14	747	0.114	−4.0
NGC 6864......	20.3	−25.8	+0.17	5	468	...	...
NGC 6934......	52.1	−18.9	+0.20	1	475	0.919	−2.0
NGC 6981......	35.2	−32.7	+0.07	1	251	1.294	−2.0
NGC 7006......	63.8	−19.4	+0.10	1	391	1.187	+0.5
NGC 7078......	65.0	−27.3	+0.12	1	332	1.346	0.0
NGC 7089......	53.4	−35.8	+0.06	1, 3	220	1.387	−1.5
NGC 7099......	27.2	−46.8	+0.06	1	214	1.767	+2.0
			RR Lyrae Stars + Abt and Golson Stars				
SW And........	115.7	−33.1	+0.058	15, 16	327	1.656	+1.5
XX And........	128.4	−23.6	+0.035	15, 16	258	1.538	+1.8
SX Aqr.........	57.9	−34.0	+0.006	15	249	1.423	−1.0
TZ Agr.........	53.2	−44.3	+0.074	15	237	1.593	+1.0
YZ Aqr.........	48.9	−49.8	+0.064	15	230	1.800	+1.5
BR Aqr.........	75.4	−55.2	+0.024	15	202	1.501	−1.0
CP Aqr.........	48.7	−31.3	+0.05	15	249	1.385	−0.2
DN Aqr........	35.7	−69.0	+0.01	16	118	...	...
341 Aql.........	45.6	−22.0	+0.034	15	401	1.017	−1.0
X Ari...........	169.1	−39.8	+0.157	15, 16	684	1.356	+2.5
TZ Aur.........	176.8	+20.9	+0.045	15, 16	331	1.493	+3.5
ST Boo.........	57.4	+55.2	−0.016	15	162	1.649	−0.5
SV Boo.........	68.8	+65.5	+0.024	15	99	1.555	−0.5
SW Boo.........	62.5	+67.8	+0.007	15	24	1.693	−0.5
TW Boo........	71.1	+62.9	+0.005	15	110	1.497	−2.0
UU Boo........	56.5	+58.0	+0.002	15	112	1.639	0.0
SS Cnc..........	198.9	+26.3	+0.113	15, 16	204	1.431	+1.0

TABLE 1—*Continued*

Object	l^{II}	b^{II}	$E(B-V)$	Source	N_H	log N_{gal}	R
TT Cnc.........	212.1	+28.4	+0.069	15, 16	248	1.476	0.0
W CVn.........	71.8	+71.0	+0.013	15, 16	44	1.700	0.0
Z CVn..........	124.0	+73.3	−0.036	15	72	1.756	0.0
RR CVn........	154.0	+81.1	−0.006	15	116	1.565	−1.0
SW CVn........	134.9	+79.8	−0.001	15	98	1.509	−2.0
SZ CVn.........	76.7	+73.7	+0.006	15	46	1.789	+0.6
RR Cet.........	143.5	−59.9	+0.024	15, 16	95	1.844	+0.6
RX Cet.........	102.4	−77.6	+0.04	16	131	1.636	0.0
RZ Cet.........	178.2	−60.4	+0.05	16	162	1.645	−1.0
S Com..........	213.1	+85.8	−0.005	15, 16	121	1.804	+0.6
RY Com........	342.4	+85.1	−0.014	15	161	1.614	−1.0
IU Car..........	269.6	−23.0	+0.08	16	361	...	...
ST Com.........	347.9	+81.3	0.00	16	142	1.591	−1.0
SU Dra.........	133.4	+48.3	+0.046	15, 16	68	1.580	0.0
AE Dra.........	84.3	+25.4	+0.023	15	272	1.373	0.0
RX Eri.........	214.3	−33.9	+0.041	15	220	1.746	−2.5
UZ Eri..........	198.9	−54.5	+0.035	15	252	1.619	+1.0
BB Eri..........	218.8	−34.4	+0.015	15, 16	175	1.942	+4.0
RR Gem........	187.4	+19.5	+0.09	15, 16	316	1.158	0.0
SZ Gem........	201.8	+22.1	+0.01	16	217	1.500	+1.0
TW Her.........	55.9	+24.8	+0.02	15, 16	298	1.459	0.0
VX Her.........	38.2	+39.1	+0.039	15	279	1.312	−1.0
VZ Her.........	59.6	+34.6	+0.026	15	267	1.516	+0.5
OX Her.........	65.2	+25.4	−0.023	15	185	1.373	−1.0
EE Her.........	32.8	+43.0	+0.003	15	195	1.675	+0.8
EP Her.........	51.9	+23.4	+0.072	15	374	1.290	+1.0
V Ind...........	355.3	−43.1	+0.06	16	146	...	...
RR Leo.........	208.4	+53.1	+0.056	15, 16	164	1.486	−1.5
RX Leo.........	209.4	+70.5	+0.017	15	77	1.842	+1.5
SS Leo..........	268.3	+57.1	+0.003	15, 16	179	1.717	+1.0
TV Leo.........	263.0	+49.1	+0.083	15, 16	197	1.730	+1.0
AA Leo.........	254.1	+66.1	+0.01	15	182	1.663	0.0
V LMi..........	201.3	+57.8	+0.028	15, 16	101	1.500	−1.5
Y LMi..........	182.5	+53.7	0.00	16	41	1.583	0.0
TT Lyn.........	176.1	+41.6	+0.014	15	124	1.465	−1.0
AQ Lyr.........	55.4	+15.2	+0.127	15	456	0.751	−1.0
IO Lyr..........	60.6	+20.0	+0.034	15	362	1.294	+0.8
KX Lyr.........	68.6	+20.4	+0.026	15	268	1.310	0.0
ST Oph.........	22.8	+16.6	+0.226	15	549	0.342	−4.0
445 Oph........	7.9	+28.5	+0.294	15	622	0.908	−2.0
452 Oph........	32.5	+25.7	+0.20	15	460	0.919	−2.0
530 Oph........	30.3	+15.3	+0.222	15	514	0.519	−4.0
531 Oph........	32.0	+15.4	+0.213	15	527	0.491	−4.0
866 Oph........	24.5	+15.5	+0.201	15	667	0.447	−2.5
VV Peg.........	78.4	−30.4	+0.013	15	252	1.507	0.0
AE Peg.........	80.2	−33.9	+0.01	15	296	1.464	0.0
AO Peg.........	69.9	−22.6	+0.036	15	276	1.072	−2.0
AV Peg.........	77.4	−24.1	+0.055	15	261	1.352	0.0
BF Peg.........	89.5	−30.4	+0.035	15	313	1.369	−1.0
CG Peg.........	77.2	−20.8	+0.074	15	272	1.301	+1.0
DZ Peg.........	93.1	−41.4	+0.019	15	176	1.714	+1.0
RY Psc.........	100.7	−62.9	+0.049	15	169	1.710	0.0
VY Ser.........	6.2	+44.1	−0.014	15	186	1.494	0.0
AN Ser.........	23.8	+45.2	+0.071	15	211	1.494	−1.0
AT Ser..........	18.1	+42.4	−0.024	15	151	1.471	−2.0
AV Ser.........	11.3	+36.8	+0.12	15	395	1.389	−0.2
AW Ser.........	28.7	+43.4	+0.008	15	178	1.787	+2.0
CS Ser..........	7.2	+45.4	+0.004	15	215	1.621	+1.0
SS Tau..........	180.1	−38.5	+0.241	15	618	1.300	+1.0
AE Tuc.........	303.2	−54.8	+0.01	16	71	...	...
AG Tuc.........	302.4	−50.4	+0.01	16	120	...	...
TU UMa........	198.8	+71.9	+0.004	15, 16	87	1.682	0.0
UU Vir.........	280.7	+60.5	−0.025	15, 16	96	1.648	0.0
UV Vir.........	286.5	+62.3	−0.007	15	119	1.544	−2.0
AS Vir..........	303.5	+52.6	+0.007	15	205	1.737	+1.0
AT Vir..........	304.6	+57.4	−0.022	15	164	1.682	+0.5
BC Vir..........	323.4	+67.5	−0.02	15	103	1.575	−1.0
BD +80°32.....	123.9	+18.6	+0.249	17	719	0.875	0.0
BD +84°02.....	122.0	+22.1	+0.112	17	300	1.587	−2.0

SOURCES.—(1) Table 1 of Burstein and McDonald 1975. (2) Quoted in Illingworth and Illingworth 1976. (3) Estimated from, or quoted in, Harris 1975. (4) Harris *et al.* 1976. (5) Table 2 of Burstein and McDonald (two-color, spectral type method) 1975. (6) Menzies 1974. (7) Cannon 1974. (8) Alcaino 1975. (9) Stetson and Harris 1977. (10) Racine and Harris 1975. (11) Walker *et al.* 1976. (12) Harris and Racine 1974. (13) Harris 1976. (14) Lee 1977. (15) Sturch 1966, 1969 + McDonald calibration. (16) Epstein and Epstein 1973 + McDonald calibration. (17) Abt and Golson 1962.

survey. The values of N_H are taken from Heiles (1976) for $\delta > -30°$ and from Heiles and Cleary (1978) for $\delta < -30°$; the units are 2.23×10^{18} cm^{-2}.

The globular cluster reddenings are both an extension and an update of Table 1 of Burstein and McDonald (1975) for clusters with $|b| > 10°$. As before, most of the globular cluster reddenings presented here were obtained by placing the independent reddening determinations from the quoted references on a common system. These independent determinations were all made without reference to the integrated properties of the clusters. In the few cases where such data were unavailable, the reddenings were obtained from the integrated color–spectral type relationship, as listed in Table 2 of Burstein and McDonald (1975). We note that there is some disagreement between the globular cluster reddenings of R. Racine, as quoted by Harris (1976), and the ones presented here; use of those other reddenings would not change the conclusions of this paper. Because of problems inherent in using the integrated properties of globular clusters to determine reddening (Burstein 1978*a*), we believe our reddenings to be the more reliable.

RR Lyrae reddenings have been obtained by using the period-color-ΔS (an Fe/H index) relationship derived by McDonald (1977) for RR Lyrae type *ab* stars at minimum light. Two separate period-color relationships, one each for halo and for old disk RR Lyrae stars (as determined from their values of ΔS), were used to obtain $E(B-V)$ from the published $(B-V)_{\min}$ colors of Sturch (1966, 1969) and Epstein and Epstein (1973), supplemented by the observations of McDonald (1977). Both the globular cluster and the RR Lyrae reddenings should be accurate, on average, to about 0.03 mag for high-latitude objects and 0.05 mag for low-latitude globular clusters (Burstein and McDonald 1975; McDonald 1977).

III. RELIABILITY OF THE $E(B-V)$ DATA: ABSENCE OF THE HEILES (1976) LATITUDE DEPENDENCE

Heiles (1976) found evidence for a latitude dependence in the relation between $E(B-V)$ and N_H, and between $E(B-V)$ and $\log N_{\rm gal}$. When the present data are used, however, the latitude dependence in the relation between $E(B-V)$ and N_H is no longer evident, as is shown in our Figure 1*a*. In Figure 1*b* there is a suggestion of a latitude dependence in the relation between $E(B-V)$ and $\log N_{\rm gal}$ for the six objects having $|b| < 20°$ and $0.13 < E(B-V) < 0.25$. However, it is unlikely that this possible dependence is significant, since four of the points lie close together in the Ophiuchus region, and are therefore not independent because $N_{\rm gal}$ is averaged over 13 deg^2. One of the other points has $b = 19\overset{\circ}{.}4$, close to the 20° boundary separating crosses and stars in the diagram.

The latitude dependence found by Heiles was the product of subtle biases in the reddening data he used. At high galactic latitudes, RR Lyrae stars predominate. The RR Lyrae reddenings used by Heiles came from Sturch (1966, 1969). These data differ in two respects from those used here. First, Sturch assumed a csc $|b|$ law with $E(B-V) = 0.03$ mag at the galactic poles; however, McDonald (1977) concludes from his analysis of RR Lyrae colors and Hβ indices that $E(B-V) = 0.00$ at the poles. This difference is reflected in the average of the reddening values for the 18 RR Lyrae stars in the original Heiles sample having $|b| > 50°$, which is 0.03 mag higher than the average for the same stars when McDonald's reddenings are used. Second, the reddenings of McDonald correct for line-blanketing effects directly, by using a $(B-V)_0$–period–ΔS relationship; in contrast, Sturch used $U-B$ as a measure of line blanketing, which introduces added error because $U-B$ is more poorly determined than is $B-V$. The large errors produced some reddenings which were negative and others which were anomalously large; the negative values were set to $E(B-V) = 0.00$ by Sturch. Therefore, the high-latitude reddening values used by Heiles were biased to higher reddenings.

At low galactic latitudes, globular clusters predominate. The globular cluster reddenings used by Heiles came from the list of Harris and van den Bergh (1974), who used an integrated color–spectral type relationship to derive $E(B-V)$. Owing to the large, possibly intrinsic scatter in this relationship (Burstein and McDonald 1975), it is possible to obtain erroneous reddenings for specific clusters. Three of the globular clusters used by Heiles lying in the range $20° < |b| < 50°$ had negative reddenings, and a fourth had a very small reddening; this biased the intermediate-latitude data toward anomalously low reddenings. (These four clusters have substantially higher positive reddenings in our Table 1.) Furthermore, the three clusters having $E(B-V) > 0.35$ had high reddenings in the compilation used by Heiles. However, the reddenings for these three clusters (NGC 6171, 6287, and 6402), as given by the sources quoted in Table 1, are in fact considerably smaller. Therefore, the low-latitude reddening values used by Heiles were biased to higher reddenings.

In summary, Heiles found a latitude dependence because of two opposite biases in the reddening data he used. We believe that our reddening data are relatively free of the biases affecting the previous list. Figures 1*a* and 1*b* lead us to conclude that there is no significant latitude dependence in the relationship of $E(B-V)$ with either N_H or $\log N_{\rm gal}$.

IV. THE VALIDITY OF GALAXY COUNTS AS AN EXTINCTION INDICATOR

The uncertainties that are encountered in evaluating galactic extinction from the reduction of galaxy counts below n_0, the average number per deg^2 expected for zero absorption, can be estimated from existing data. The fractional uncertainty due to Poisson variation is $n_0^{-1/2}$ and would amount to 14% for the actual count $n_0 \approx 50$ in the galactic caps; at $|b| = 20°$, where only about $\frac{1}{3}$ as many galaxies were counted, it would be 25%. The corresponding values of the error due to the Poisson variation in $\log N_{\rm gal}$, $\sigma_P(\log N_{\rm gal})$, would be 0.06 and 0.10, respectively. However, this is considerably less than the total

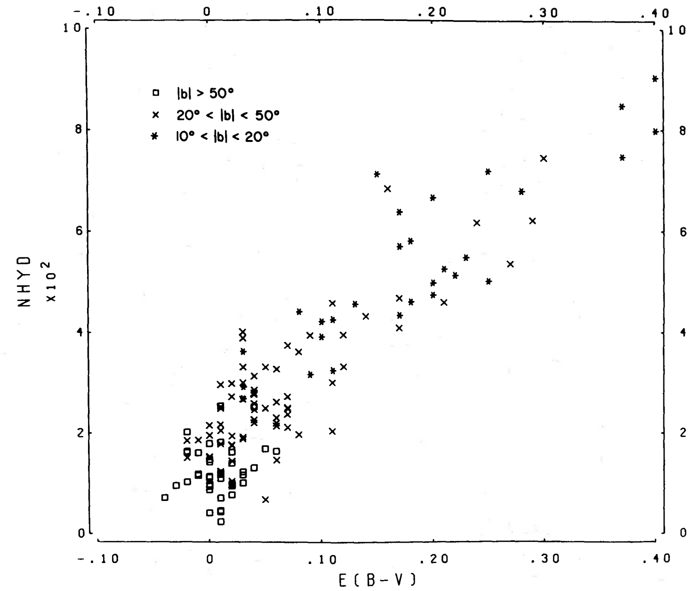

FIG. 1a

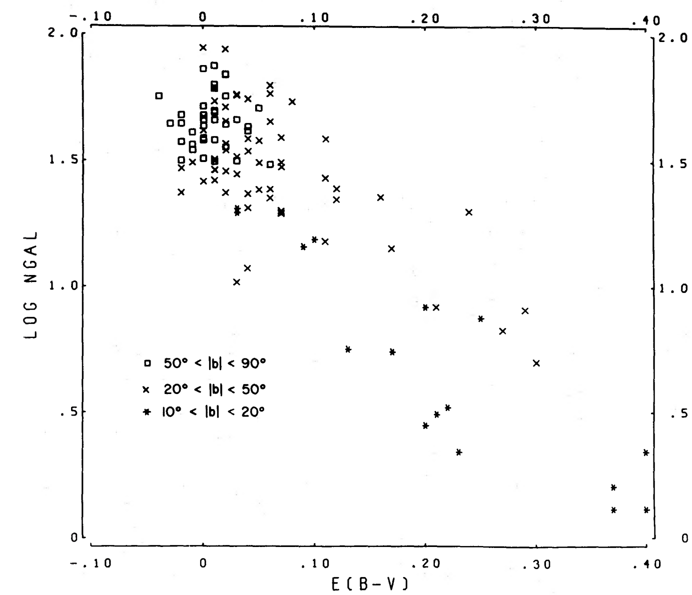

FIG. 1b

FIG. 1.—(a) N_H versus $E(B - V)$ for all objects in Table 1. Squares have $|b| > 50°$; crosses have $20° < |b| < 50°$; stars have $10° < |b| < 20°$. (b) Log N_{gal} versus $E(B - V)$ for all objects in Table 1 having SW galaxy counts. In this figure, N_{gal} has been averaged over a 13 deg² area centered on the object. The meanings of the symbols are as for Fig. 1a.

uncertainty. Over the north polar galactic cap Heiles (1976) found the total rms variation in $\log N_{gal}$, $\sigma_T(\log N_{gal})$, to be 0.15; thus $\sigma_P/\sigma_T \approx 0.43$ at high latitudes. Because uncorrelated errors add in quadrature, Poisson statistics are unimportant in increasing σ_T for $|b| \gtrsim 20°$.

This excess of σ_T over σ_P cannot result from counting or correction errors in the SW analysis. From a statistical study of overlap zones in the SW counts, Seldner *et al.* (1977) found that the rms fractional error in the correction factors used by SW to reduce all plates to a uniform standard was 6% of n_0, equivalent to only $0.18\sigma_T$. A similar analysis by Groth and Peebles (1977) showed that the SW counting errors amounted to increasing the Poisson variation by 15%, equivalent to only $0.06\sigma_T$. Since these errors are uncorrelated with each other or with the purely statistical error σ_P, they add in quadrature and therefore only contribute a relatively minor amount to the total uncertainty.

Variations in the diffuse sky brightness have been suggested as affecting the SW counts. As discussed below, recognition of a galaxy as being different from a star involves the threshold surface brightness in the image profile, not the apparent magnitude of the galaxy. From statistical considerations, we expect the detectable threshold of a galaxy to increase as the square root of the background brightness level divided by the area over which the galaxy is brighter than the threshold. Since the area of a galaxy increases with decreasing surface brightness, the threshold should vary more rapidly than the square root of the background level—say, as (background)^x, where $x > 0.5$. This provides Δm(threshold) = $x\Delta\mu$(sky), where Δm is the variation in detectable threshold caused by $\Delta\mu$(sky), the variation of the surface brightness of the sky in magnitude units. Airglow and artificial illumination are the largest contributors to the sky brightness (Roach and Gordon 1973) and would affect Δm(threshold) to the extent that they vary with time and position. Zodiacal light is comparable in intensity and is concentrated toward the ecliptic plane, which passes near the north galactic pole; variations in the zodiacal light within the polar cap would contribute to the value of σ_T found by Heiles. If resolved stars to $m_{pg} \leq 19$ are excluded, then according to Roach and Gordon (1973) the variations in zodiacal light over the surveyed declinations will change the residual sky brightness by about ± 0.4 mag, and Δm(threshold) by $\pm 0.4x$ mag. Since $\gamma = 1$ (Heiles 1976; and the discussion below), this corresponds to a variation in $\log N_{gal}$ of $0.4x$. Since $x > 0.5$, this quantity is larger than $\sigma_T = 0.15$. Galactic light (Roach and Gordon 1973) would affect the zones $10° < |b| < 20°$ even further; at $|b| = 15°$ the sky brightening would change Δm(threshold) by about 0.1 mag, which is somewhat less than the contribution from zodiacal light.

Thus sky brightness effects would have been important if the plates had been sufficiently exposed so that the sky brightness was detected. However, they were not (Klemola 1977), and variations in sky brightness could not have contributed to σ_T except near diffuse nebulae such as galactic H II regions.

Crowding of galactic stars at low galactic latitudes has often been suggested as a reason for the loss of an appreciable fraction of otherwise recognizable galaxies (Knapp and Kerr 1974). McGillivray (1975) found that, in the environs of 47 Tuc, crowding losses became appreciable when there were more than 20,000 stars deg^{-2}. At the limiting magnitude $m_{pg} = 19.3$ for the Lick astrograph, the star count tables (Allen 1976), corrected by 0.5 mag for the error in the Seares magnitude scale (Stebbins, Whitford, and Johnson 1950), predict about 12,000 stars deg^{-2} at $|b| = 10°$. Checks of typical astrograph plates like those used by SW are consistent with this density. Therefore, crowding losses appear to have had little influence on the SW counts, unless the personal equation of the individuals performing the counting involves the star density.

We conclude that, over most of the sky, the major component in the total $\sigma_T = 0.15$ is the intrinsic mottling in the surface density of the distribution of galaxies. This unevenness, apparent in the SW maps of counts smoothed over 4 deg^2, is even more striking in the photographic representation of the 1 deg^2 counts (Heiles and Jenkins 1976) or the 10′ squares (Seldner *et al.* 1977). Heiles (1976) found that the scatter of correlation plots was reduced by averaging $\log N_{gal}$ over 13 deg^2. A reduction by a factor $13^{1/2}$ was not realized because adjacent areas are not random but are correlated with declining importance out to a radius of about 2°.5 (Groth and Peebles 1977). Smoothing over 13 deg^2 does reduce the purely statistical part of the uncertainty; at $|b| = 20°$, σ_P is reduced from 0.10 to 0.03. A reasonable estimate of the total uncertainty (statistics, counting errors, clumping tendency) would probably be a reduction of σ_T from about 0.15 to 0.1, if $\log N_{gal} \gtrsim 0.7$. This estimate is borne out by the correlation plots in the present paper, i.e., Figure 1*b*.

The theoretical value $\gamma = 0.47$ derived by SW assumed that extinction affects galaxy images near the counting limit in the same way that it does stars. The empirical value $\gamma = 1.0$ determined by calibrating actual counts against known extinction differences (Heiles 1976) supports the contention that the recognition of a galaxy as being different from a star involves a threshold surface brightness in the image profile, not merely the detection of an image of any kind (e.g., Neckel 1965). Furthermore, the least-squares fit to the data presented in Figure 1*b* yields $\log N_{gal} = (1.645 \pm 0.024) - (3.62 \pm 0.21)E(B-V)$, consistent with $\mathscr{R} = 3.6$ if $\gamma = 1.0$; this is close to $\mathscr{R} = 4.0$, which is the generally accepted value. In contrast, $\gamma = 0.47$ would provide $\mathscr{R} = 7.7$. We believe that the available evidence favors $\gamma = 1.0$, which is the value we shall adopt for our discussion. However, we note that there is no reason to expect γ to be independent of A_{pg}, for the reasons noted by Heiles (1976); thus any value adopted can be only a representative one averaged over some appropriate range of A_{pg}. Accurate determination of the reddenings of many more objects outside of the galactic absorbing layer will be needed, however, to establish any such dependence of γ on A_{pg}.

V. GALAXY COUNTS AND THE EXTINCTION AT HIGH GALACTIC LATITUDES

Previous analyses of the SW galaxy counts (SW; Heiles 1976) as well as analyses of other galaxy and galaxy cluster counts (e.g., de Vaucouleurs and Malik 1969; Holmberg 1974) imply a polar photographic extinction of about 0.25 mag. This is considerably larger than the values derived from photometric studies of reddening at high galactic latitude (e.g., the references cited in Paper I and in Burstein and McDonald 1975), which indicate that the reddening near the poles is irregularly distributed between values of 0.00 and 0.03 mag in $E(B-V)$. The zero-point offset and variable gas-to-dust ratio, to be discussed in § VI, make N_H useless for resolving the discrepancy.

We now resolve this discrepancy by a reanalysis of the galaxy counts, using a new technique for obtaining the average value of N_{gal}.

Past galaxy count analyses have averaged all galaxy counts within a given latitude range, obtaining the mean value of log N_{gal} as a function of csc $|b|$. However, these mean values of log N_{gal} are determined both by extinction in our Galaxy and by variations in the intrinsic, large-scale mottling of the galaxy counts themselves (see § IV). Near the galactic poles, these mottling variations can become important in the determination of the mean value of log N_{gal}, since, for $|b| > 60°$, latitude bins subtend a relatively small angular size on the sky. In particular, the polar regions are susceptible to variations in the mean value of log N_{gal} due to the presence of large, relatively nearby clusters (e.g., those in the Local Supercluster) whose angular distribution is not averaged out over the sky.

The problem of how best to determine an "average" value of log N_{gal} as a function of b is somewhat analogous to the problem of how best to determine the average sky background in a field of stars on a photographic plate. Borrowing a technique developed for the latter problem (Burstein 1978*b*), we plot the histogram of the number of "picture elements" (pixels) with log N_{gal} between N and $N + \Delta N$. These picture elements are those used by Heiles and Jenkins (1976), which are smaller than the 1 deg^2 elemental areas of the SW survey; thus the number of pixels is larger than the number of independent data points in each histogram. For the intervals in csc b = 0.02, 1 pixel = 0.09 deg^2; for the other intervals, 1 pixel = 0.18 deg^2.

If all latitude intervals were equally affected by mottling and had little variation in extinction within them, then all of the histograms would be similar in appearance. They would appear symmetric, with a half-width of approximately 0.15 in log N_{gal} (§ IV) and with the position of the peak of the distribution determined by the average extinction in that latitude interval. If large-scale clustering, in excess of the average, is present within a latitude bin, the larger number of pixels with high values of log N_{gal} will distort the histogram in that direction. Conversely, if there is substantial variation of extinction within the latitude interval, then the histogram will be distorted toward low values of log N_{gal}. Any combination of these effects will produce a broad or ill-defined histogram.

Note that, if a cluster occupies the whole area covered by a histogram, it will produce a symmetric histogram having an anomalously high value of log N_{gal} instead of a histogram having abnormally long tails.

Figures 2*a* and 2*b* plot the histograms for the north galactic pole (NGP) and the south galactic pole (SGP) regions, in intervals of 0.02 in csc b, from csc $|b|$ = 1.00 to csc $|b|$ = 1.16. The histograms are noisy, but several properties of these data are apparent: (*a*) Most of the NGP and some of the SGP histograms are primarily Gaussian in shape; (*b*) some histograms have an extra bump at large values of log N_{gal} (e.g., csc b = 1.00–1.02; csc b = 1.08–1.10); (*c*) histograms can vary in half-width from Δ log N_{gal} = 0.12 to Δ log N_{gal} = 0.20; (*d*) some histograms have broad, flat maxima, others have sharp maxima, while one

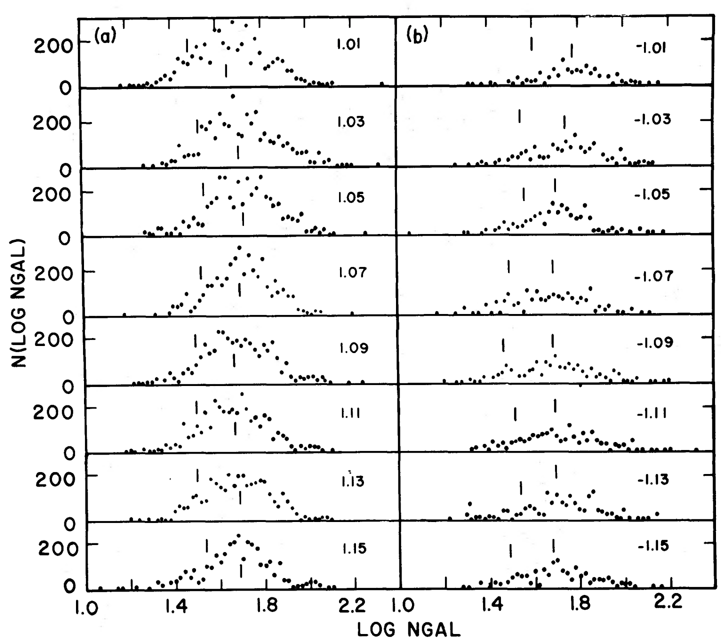

FIG. 2.—Histograms for the SW galaxy counts near the galactic poles, plotted as the number of pixels with log N_{gal} between N and $N + \Delta N$, versus log N_{gal}. (*a*) North galactic polar region; (*b*) south galactic polar region. The center of each csc interval is given, and the values of log $N_{gal}(C)$ and log N_{gal}(HW) are denoted by vertical lines.

TABLE 2

VALUES OF log N_{gal}, FROM HISTOGRAM METHOD, AS A FUNCTION OF csc b

csc Interval	No. of Pixels	log N_{gal} (C)	log N_{gal} (HW)
+1.00 to +1.02...	4498	1.65 ± 0.05	1.48 ± 0.05
+1.02 to +1.04...	4356	1.70 ± 0.06	1.52 ± 0.06
+1.04 to +1.06...	4260	1.72 ± 0.05	1.54 ± 0.05
+1.06 to +1.08...	4048	1.70 ± 0.05	1.53 ± 0.05
+1.08 to +1.10...	3996	1.67 ± 0.05	1.50 ± 0.05
+1.10 to +1.12...	3869	1.67 ± 0.05	1.50 ± 0.05
+1.12 to +1.14...	3706	1.69 ± 0.05	1.50 ± 0.05
+1.14 to +1.16...	3403	1.69 ± 0.04	1.54 ± 0.04
+1.13 to +1.20...	13200	1.68 ± 0.05	...
+1.21 to +1.31...	13219	1.62 ± 0.05	...
+1.32 to +1.47...	13200	1.58 ± 0.05	...
+1.48 to +1.69...	12568	1.56 ± 0.05	...
+1.70 to +2.03...	11067	1.48 ± 0.06	...
+2.04 to +2.56...	10386	1.36 ± 0.08	...
+2.57 to +3.56...	9691	1.22 ± 0.08	...
+3.57 to +5.75...	8488	0.74 ± 0.16	...
−1.00 to −1.02...	1305	1.78 ± 0.06	1.60 ± 0.06
−1.02 to −1.04...	1836	1.75 ± 0.06	1.55 ± 0.06
−1.04 to −1.06...	1919	1.71 ± 0.05	1.57 ± 0.05
−1.06 to −1.08...	1889	1.69 ± 0.06	1.50 ± 0.06
−1.08 to −1.10...	1911	1.69 ± 0.05	1.47 ± 0.05
−1.10 to −1.12...	1877	1.70 ± 0.04	1.52 ± 0.04
−1.12 to −1.14...	1828	1.70 ± 0.05	1.54 ± 0.05
−1.14 to −1.16...	1680	1.68 ± 0.04	1.49 ± 0.04
−1.13 to −1.20...	6865	1.68 ± 0.05	...
−1.21 to −1.31...	7046	1.60 ± 0.05	...
−1.32 to −1.47...	7477	1.62 ± 0.08	...
−1.48 to −1.69...	7402	1.55 ± 0.08	...
−1.70 to −2.03...	7569	1.47 ± 0.08	...
−2.04 to −2.56...	7574	1.32 ± 0.12	...
−2.57 to −3.56...	7791	1.18 ± 0.12	...
−3.57 to −5.57...	7570	0.62 ± 0.16	...

appears to have two separate maxima (csc b = 1.04–1.06). All of these effects can be understood in terms of galaxy clustering and of variation in the extinction within latitude bins.

We wish to minimize the effects of excess, large-scale clustering, in order to derive relatively unbiased values of log N_{gal} with which to investigate the variation of extinction with latitude. Gaussians could be fitted to these histograms, but it is not clear that these histograms should necessarily be intrinsically Gaussian in shape. Instead, two other methods were used: (1) Choose the point midway between the half-power points of the central maximum of the histogram [= log $N_{gal}(C)$]; (2) choose the value of log N_{gal} at the half-power point toward smaller values of log N_{gal} [= log N_{gal}(HW)]. [In practice, the value of log $N_{gal}(C)$ and that determined by a Gaussian fit are essentially the same.] Both estimates of log N_{gal} are listed in Table 2 for this latitude range, along with the total number of pixels in each latitude interval. These estimates are plotted versus csc $|b|$ in Figures 3a and 3b.

A further advantage of the histogram method is that it provides an independent, realistic estimate of the error in log N_{gal}(average); we estimate the error to vary from 0.04 to 0.06 in log N_{gal} for csc $|b|$ = 1.00–1.16. These error estimates are given in Table 2 and plotted in Figure 3. As a check on the reliability

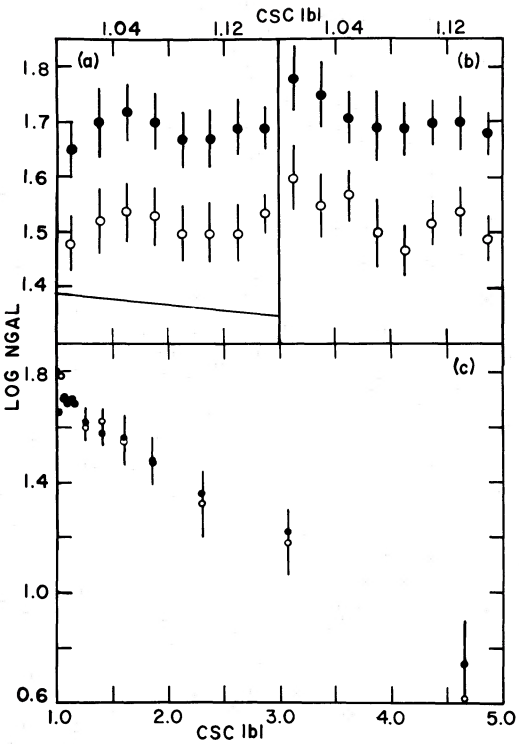

FIG. 3.—The average value of log N_{gal}, as determined from the histogram method, versus csc $|b|$, from Table 2. (a) NGP region: Filled circles are log $N_{gal}(C)$, and open circles are log N_{gal}(HW); a slope corresponding to a csc law coefficient of 0.25 mag is given. (b) SGP region: Symbols are the same as in Fig. 3a. The galaxy count data, as evidenced by Figs. 3a and 3b, are too noisy to allow one to discriminate between csc law coefficients of 0.00 and 0.25. (c) Log $N_{gal}(C)$ versus csc $|b|$ for the SW counts: Filled circles have $b > 10°$; open circles have $b < -10°$.

of the histogram method of determining log N_{gal}, Table 2 lists, and Figure 3c plots, log $N_{gal}(C)$ versus csc $|b|$ for the rest of the SW data, in csc intervals as noted in Table 2. Comparison of this figure with the analogous figure in Heiles (1976) shows little difference between the two figures for csc $|b| < 1.5$.

For the NGP, log N_{gal} exhibits little systematic variation with csc $|b|$; indeed, a least-squares fit to the data gives a positive (i.e., log N_{gal} *decreasing* toward the pole) coefficient of csc $|b|$ of 0.03 ± 0.16. However, the SGP measurements indicate that log N_{gal} increases substantially toward the south galactic pole. Inspection of the SW maps shows that much of the area very near the SGP is influenced by four large clusters, which cause the value of log N_{gal} to increase for csc $b > -1.03$. Three additional points argue that the increase in log N_{gal} near the SGP is due to statistical fluctuations in galaxy clustering: (1) At csc $|b|$ = 1.00–1.02, the value of log N_{gal} at the SGP is 0.13 higher than at the NGP, so that either the SGP has 0.03 mag less reddening than the NGP or log N_{gal} can vary widely (e.g., by 0.13, in agreement with the estimates of § IV); (2) the slope of the csc law at the SGP predicts $E(B-V) = 0.15$ csc $|b|$, a rather large amount of reddening at the SGP and contradictory to point 1; (3) the number of pixels in the SGP averages are $\frac{1}{2}$ to $\frac{1}{3}$ the number in the NGP and are spread over a considerably smaller range in longitude, thereby leaving the SGP histograms more susceptible to clustering perturbations.

We conclude that the possible systematic trends of $\log N_{\mathrm{gal}}$ with $\csc b$, in this restricted latitude range near the poles, are not significant. Even for the SGP, the errors in $\log N_{\mathrm{gal}}$ are too large to enable us to distinguish between csc law coefficients of 0.00 and 0.15 in $E(B - V)$. These data show explicitly that the galaxy counts alone cannot be used to argue that there is either reddening or extinction at the poles, or that a linear csc law is valid up to the poles. *The galaxy count data are too noisy to determine the slope of a csc law near the galactic poles.*

The same statement is true for the Zwicky galaxy cluster data, as analyzed by Holmberg (1974). With 1927 clusters in 48 fields (for $b > 63°$), the variation in $\log N_{\mathrm{clust}}$, per field, due to Poisson statistics (cf. § IV) is $\sigma = 0.06$. From the map given by Holmberg (1974), one can plot the histogram of $\log N_{\mathrm{clust}}$ for $b > 60°$ for the individual fields (analogous to the similar plot made by Heiles 1976 for the SW counts). This histogram has an approximate half-width of $\sigma_T = 0.15$ in $\log N_{\mathrm{clust}}$. As with the SW counts, $\sigma_T \gg \sigma_P$, which shows that the galaxy cluster counts of Zwicky are as affected by mottling as are the SW counts. For $\csc b = 1.00$ to $\csc b = 1.10$, the average dispersion in the galaxy cluster counts [the value of $\epsilon(\Delta A)$ in Table 2 of Holmberg 1974] is too large to allow one to discriminate between no change in $\log N_{\mathrm{clust}}$ as a function of $\csc |b|$ and a change corresponding to a csc law slope of $A_{\mathrm{pg}} = 0.25 \csc b$.

Thus we have shown that the weight of evidence in the distribution and amplitude of reddening at the galactic poles has to come from the photometric studies of stars, globular clusters, or galaxies. The analysis of galaxy counts can place only a rather weak constraint on the distribution of reddening at the galactic poles.

Holmberg (1974) introduced a discussion of a possible zero-point error in the photometric data, because these data conflicted with his reddening value for the NGP as determined from Zwicky galaxy cluster counts. In light of the above discussion, the assumption of such a zero-point error is unwarranted. Furthermore, both the Hilditch, Hill, and Barnes (1977) A and F star reddenings on the Strömgren system (as well as the other A and F star investigations quoted therein) and the McClure and Crawford (1971) K giant reddenings on the DDO system are calibrated with a sufficient number of nearby standards to be free of zero-point reddening errors; and both photometric systems can detect differences in metallicity and luminosity.

We therefore conclude that there is little or no reddening at the NGP. All available data, including those from the analysis of galaxy counts, are consistent with this conclusion. The patchy reddening distribution at the NGP is perhaps best given by Hilditch *et al.*; there may be somewhat more reddening, again irregularly distributed, at the SGP (as implied by the N_{H} maps of Heiles 1975).

VI. THE GAS-TO-DUST RELATION

a) The Variable Gas-to-Dust Relation, as Derived from N_{gal} and N_{H}

Even though the relation between galaxy counts and extinction has some residual uncertainty (see § IV), the relation between galaxy counts and hydrogen column density can be useful in illuminating some aspects of the gas-to-dust relationship. In particular, it is useful in probing the *variability* of this relationship.

We have searched for possible variation in the gas-to-dust ratio with longitude by fitting, in the least-squares sense, equations of the form

$$\log N_{\mathrm{gal}} = A + BN_{\mathrm{H}} \tag{1}$$

for 30 intervals of galactic longitude, each 12° wide (eqs. [1]–[3] were derived from data on the whole sky, not just from the data in Table 1). For consistency with the results of Heiles (1976), we included only points having $|b| > 20°$, $N_{\mathrm{H}} > 200$, and $\log N_{\mathrm{gal}} > 0$; and we excluded points with $|b| > 64°$ in addition, for purposes of computational convenience. We have also fitted equations with the left-hand side of equation (1) containing the additive term $0.203 \csc |b|$, again following Heiles (1976), and have obtained solutions including the larger latitude range $10° < |b| < 64°$. These modifications make minor quantitative differences in the results but do not change our conclusions.

A and B are plotted versus the intervals of longitude in Figures 4*a* and 4*b*. In examining these figures, one should remember that the longitude interval 250°–360° at positive latitudes is covered only at the higher latitudes, owing to the southern declination limits of the galaxy counts; thus the range in $\csc |b|$, and also in N_{H} and $\log N_{\mathrm{gal}}$, is restricted so that the errors are larger than usual. These figures show that the zero point A has modest variation with longitude. However, the slope B has very large variations, even changing sign in the most extreme circumstances. The natural conclusion from these figures is that the gas-to-dust ratio is variable. With a representative value of A, the ratio $(\log N_{\mathrm{gal}} - A)/N_{\mathrm{H}}$ also varies among $12° \times 12°$ bins by large amounts, which supports this conclusion. The statistical error associated with the points in Figure 4*b* is very small. However, the true errors are likely to be systematic instead of random and, although probably small, cannot be estimated from the present data.

One other possible way to obtain the results in Figure 4*b* could occur if $\log N_{\mathrm{gal}}$ varied with latitude independent of N_{H}; for example, if $\log N_{\mathrm{gal}} = C + D \csc |b| + EN_{\mathrm{H}}$, as found by Heiles (1976). Since, at least to a crude approximation, we typically have

$$N_{\mathrm{H}} = F + G \csc |b| \tag{2}$$

for all of the longitude regions (Fejes and Wesselius

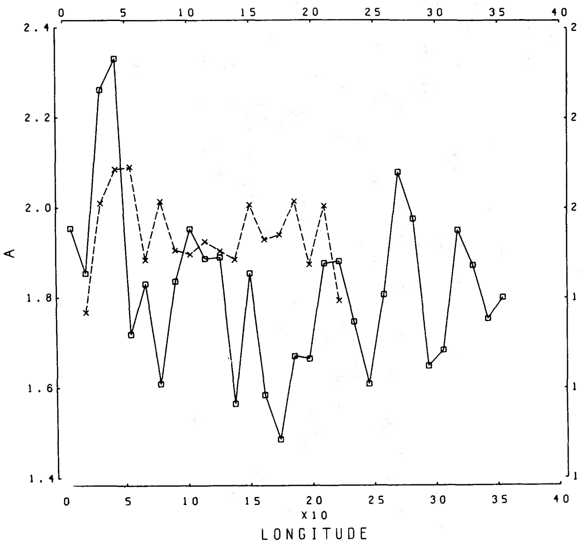

FIG. 4*a*

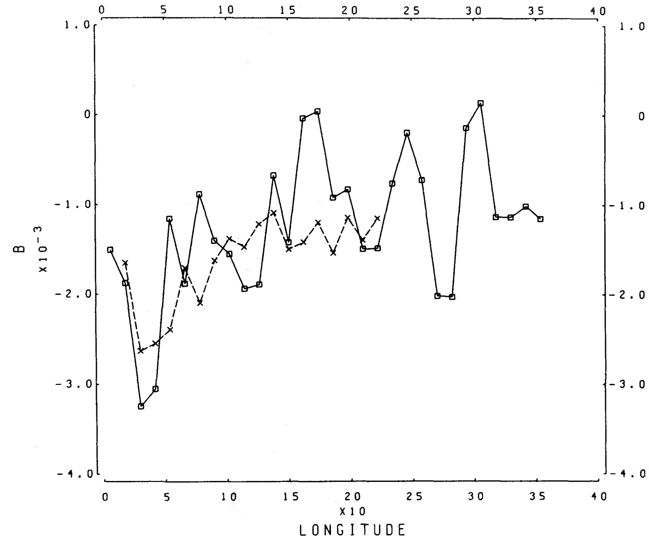

FIG. 4*b*

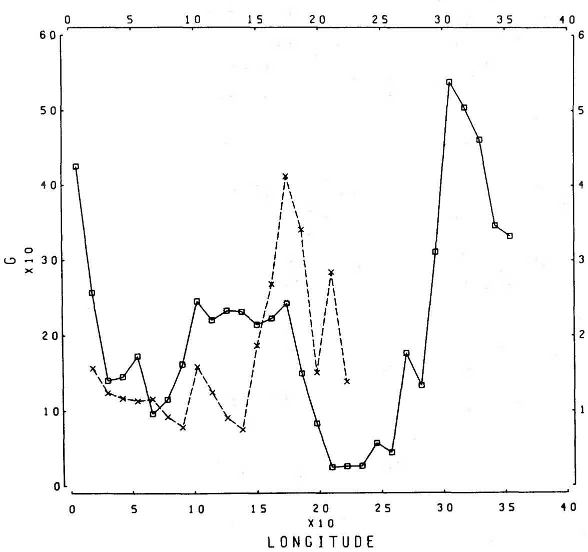

FIG. 4*c*

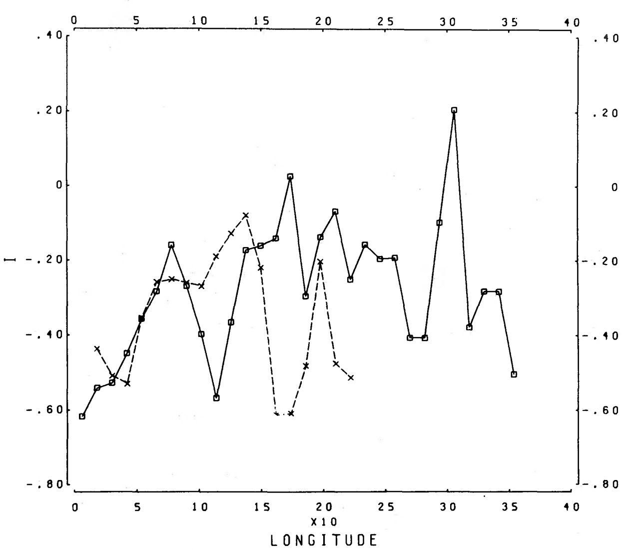

FIG. 4*d*

FIG. 4.—(*a*) A in eq. (1) versus longitude. Least-squares fits were made for data in 12° wide bins of longitude, as explained in the text. Squares joined by the solid line have $20° < b < 64°$; crosses joined by the dashed line have $-64° < b < 20°$. (*b*) B in eq. (1) versus longitude. The meanings of the symbols are the same as for Fig. 4*a*. *Abscissa*, longitude $\times 10$; *ordinate*, $B \times 10^{-3}$. (*c*) G in eq. (2) versus longitude. The meanings of the symbols are the same as for Fig. 4*a*. *Abscissa*, longitude $\times 10$; *ordinate*, $G \times 10$. (*d*) I in eq. (3) versus longitude. The meanings of the symbols are the same as for Fig. 4*a*.

1973), with G a function of longitude, we have $\log N_{\rm gal} = (C - DF/G) + (E + D/G)N_{\rm H}$, i.e., with the coefficient of $N_{\rm H}$ in equation (1) a function of longitude even with no variation in the gas-to-dust ratio. In Figure 4*c* we plot the variation of G with longitude; if this is the source of the variation in B, we should always have B large with G small. There are some trends in this direction, which probably indicates that a separate $\csc |b|$ dependence of $\log N_{\rm gal}$ does exist; however, the variability in the gas-to-dust ratio, embodied in the coefficient B, is clearly present as well.

A different way to show the variability in the gas-to-dust ratio is to examine the longitude dependence of the factor I in the equation

$$\log N_{\rm gal} = H + I \csc |b| \quad (3)$$

and, in particular, the correlation between G and I. The variation of I with longitude is presented in

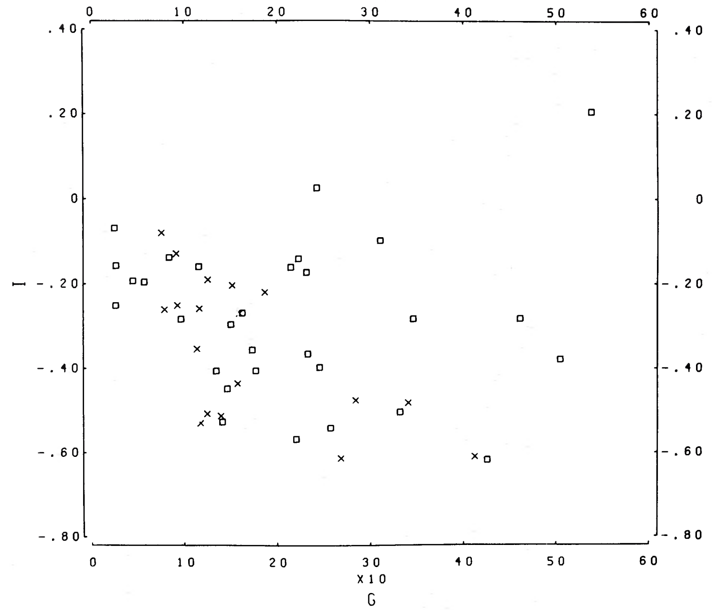

FIG. 5.—I in eq. (3) versus G in eq. (2) for the 12° wide longitude bins displayed in Fig. 4. Squares have $20° < b < 64°$; crosses have $-64° < b < -20°$.

Figure 4d, and individual points of G and I are plotted in Figure 5. While there is a trend for I to decrease with increasing G, as expected for a constant gas-to-dust ratio, there is much scatter in the relation.

We conclude that the gas-to-dust ratio does vary with position on the sky. In Heiles (1976), this variation was seen primarily as a latitude variation in the log $N_{\rm gal}$ to $N_{\rm H}$ ratio; here we have shown explicitly that it is a function of both latitude and longitude. Qualitatively similar effects were noted by Seki (1973).

b) New Methods for Predicting Reddening Based on the Variable Gas-to-Dust Ratio

Figure 4 shows the longitude behavior of the gas-to-dust ratio, averaged over considerable areas in the sky. For the purpose of predicting the extinction, it would be desirable to have information on the variation on smaller angular scales.

Though both the galaxy counts and the H I column densities show a good average correlation with extinction, each is subject to local variations. The counts are affected by clustering, which is reduced but not eliminated by smoothing over a 13 deg^2 area. Use of the histogram method (§ V) to determine the 13 deg^2 log $N_{\rm gal}$ average would not give a significantly different result, since 13 deg^2 is not a large enough area of the sky and does not contain many pixels. The ratio of reddening to $N_{\rm H}$ depends on variations in the gas-to-dust ratio. Since there is no reason to suppose that galaxy clustering should be correlated in position with the variability of the gas-to-dust ratio, a more reliable prediction of reddening should come from a combination of the two sets of observations than from either one alone. We have therefore proceeded on the basis of using the relation between log $N_{\rm gal}$ and $N_{\rm H}$, as a function of position, to correct the average slope in the gas-to-dust ratio.

With the currently available data, one can form the relationship among $E(B-V)$, $N_{\rm H}$, and log $N_{\rm gal}$ in two ways. In the first way, we take the residuals from the average relation between log $N_{\rm gal}$ and $N_{\rm H}$, presented in Figure 9 of Heiles (1976), as measures of the departures from the average gas-to-dust ratio. We fit in the least-squares sense the coefficients x_1, x_2, and x_3 in the equation

$$E(B-V) = x_1 + x_2 N_{\rm H} + x_3 R N_{\rm H} \tag{4}$$

to the reddening data in Table 1.[1] Here R is the residual in Heiles's contour units (e.g., a residual of 0.1 in log $N_{\rm gal}$ has $R = 1.0$); $N_{\rm H}$ is obtained from Heiles (1975), where it is mapped as a function of galactic coordinates.

If one substitutes for R in equation (4), using the definition of R in equation (3) of Heiles (1976), one obtains (ignoring the terrestrial atmospheric extinction term)

$$E(B-V) = y_1 + y_2 N_{\rm H} + y_3 N_{\rm H}^2 + y_4 N_{\rm H}(\log N_{\rm gal}) + y_5 N_{\rm H}(\csc|b|)\,. \tag{5}$$

The csc $|b|$ term in equation (5) dominates the

[1] We note that, according to the definition of the residual in Fig. 9 of Heiles (1976), it would have been more consistent to fit an equation of the form $E(B-V) = A + BN_{\rm H} + CR$. However, this equation produced significantly higher residuals than did eq. (4). In this case, we consider the empirical result to be superior.

TABLE 3

LEAST-SQUARES FITS

a) Least-squares fit to eq. (4):*

$$E(B-V) = \underset{\pm 0.0058}{-0.0372} + \underset{\pm 0.020}{0.357} \times 10^{-3}N_{\rm H} - \underset{\pm 0.062}{0.346} \times 10^{-4}RN_{\rm H}$$

Weighted mean error = 0.032 mag
Mean error of globular clusters = 0.026
Mean error of RR Lyrae stars = 0.035

b) Least-squares fit to eq. (6):

$$E(B-V) = \underset{\pm 0.0092}{-0.0171} + \underset{\pm 0.090}{0.399} \times 10^{-3}N_{\rm H} + \underset{\pm 0.097}{0.140} \times 10^{-6}N_{\rm H}^2 - \underset{\pm 0.034}{0.126} \times 10^{-3}N_{\rm H}\log N_{\rm gal}$$

Weighted mean error = 0.0326
Mean error of globular clusters = 0.0322
Mean error of RR Lyrae stars = 0.0328

* NGC 6287, 6333, 6356, and 6402, with $|b| < 15°$, have been excluded from the fit.

$N_{\rm H}(\log N_{\rm gal})$ term for csc $|b|$ large. Since this csc $|b|$ term exists only because of the original formulation in Heiles (1976), a more correct formulation, to account for variation in the gas-to-dust ratio, would be to have equation (5) without the csc term, viz.,

$$E(B-V) = y_1 + y_2N_{\rm H} + y_3N_{\rm H}^2 + y_4N_{\rm H}(\log N_{\rm gal}) . \quad (6)$$

The first formulation (eq. [4]) was presented because of the availability of maps for both $N_{\rm H}$ and R. A comparison of the two methods for the data in Table 1 shows that both give the same result for values of $|b| > 15°$ and/or $E(B-V) < 0.3$. Below $|b| = 15°$, equation (4) is probably less accurate than what would be obtained by using equation (6). The results of the fits of equations (4) and (6) are shown in Figures 6*a* and 6*b*, and the values of the coefficients and other data concerning the quality of these fits are presented in Table 3.

Some care was taken in determining the best fits for both equations. First, for equation (4) we excluded four globular clusters which had $|b| < 15°$, for the reason given above. To account for any possible difference in the random errors of the two main classes of objects (globular clusters and RR Lyrae stars), each class was weighted differently in each fit, by weights inversely proportional to the squares of the mean errors from the fit of the objects in each class (see Table 3). Several iterations of each fit were performed in order to be sure that the weighting and the residuals were indeed correct.

The average of the mean errors of the globular clusters to the fits to equations (4) and (6) is 0.028 mag in $E(B-V)$; for the RR Lyrae stars this is 0.034 mag. The globular cluster mean error is comparable to the expected measurement errors for the cluster reddenings. Examination of Figure 6 shows that the scatter increases with reddening, which is *a priori* expected for the measurement errors in globular cluster reddenings (Burstein and McDonald 1975). Apparently, the measurement errors contribute much to the mean errors from our fits. Under these circumstances, it is difficult to estimate the intrinsic accuracy of our fit. The mean error of an individual prediction using equation (4) or equation (6) would appear to be less than 0.03 mag in $E(B-V)$.

Galaxy clustering, which produces random errors in the value of R, still affects the values of $E(B-V)$ derived from equations (4) and (6). However, the galaxy counts are used only to make a (usually) relatively small change in the slope of the gas-to-dust relation. As discussed briefly in Paper I, clustering should not often produce errors in R larger than about 1; for $N_{\rm H} = 500$, corresponding to $E(B-V) = 0.14$ mag, this corresponds to an error of only 0.02 in $E(B-V)$. A comparable error is expected for equation (6). Of course, the absolute size of the error is smaller for points with smaller $N_{\rm H}$.

Setting either x_3 in equation (4) or y_4 and y_3 in equation (6) equal to zero is equivalent to assuming a constant gas-to-dust ratio. The difference in the zero-point coefficients x_1 and y_1 arises because, for $|b| > 60°$, the $y_3N_{\rm H}^2$ term is negligible compared to the $y_4N_{\rm H}(\log N_{\rm gal})$ term in equation (6), and the $y_4N_{\rm H}(\log N_{\rm gal})$ term is approximately constant and equal to -0.02. This, taken together with y_1, is roughly equal to the value of x_1 in equation (4). In order to use equation (6) to determine $E(B-V)$, the value of $\log N_{\rm gal}$, smoothed to 13 deg^2, is needed. A map of $\log N_{\rm gal}$, smoothed to 4 deg^2, is given by SW; further smoothing to 13 deg^2 can be accomplished by the use of this map.

By assuming a constant gas-to-dust ratio, one obtains

$$E(B-V) = z_1 + z_2N_{\rm H} . \quad (7)$$

A least-squares fit to equation (7) for all of the data presented in Figure 1*a* yields coefficients $z_1 = -0.055 \pm 0.006$ and $z_2 = (0.443 \pm 0.018) \times 10^{-3}$, with a mean error of 0.040 mag, considerably larger than the mean errors for the fits to equations (4) and (6). The mean errors and derived values of z_1 and z_2 are not changed by the removal of the southern data from the fit. The mean error, by including only those points used in the fit to equations (4) and (6) and by

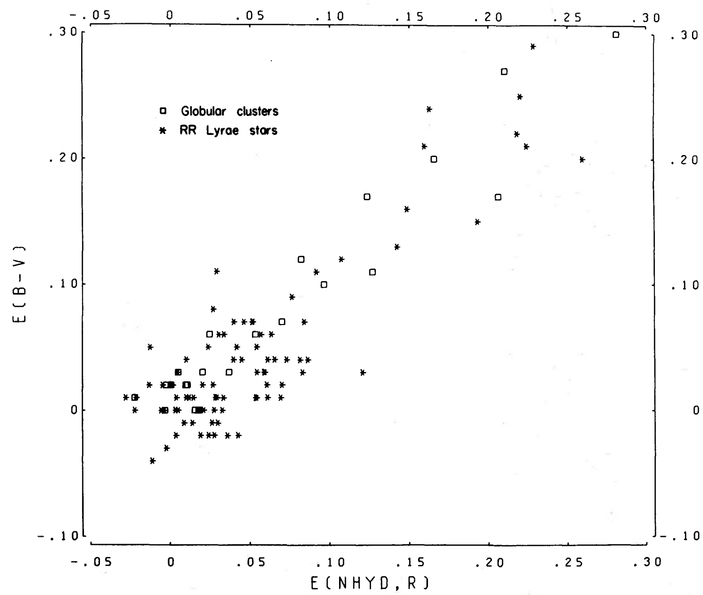

FIG. 6*a*

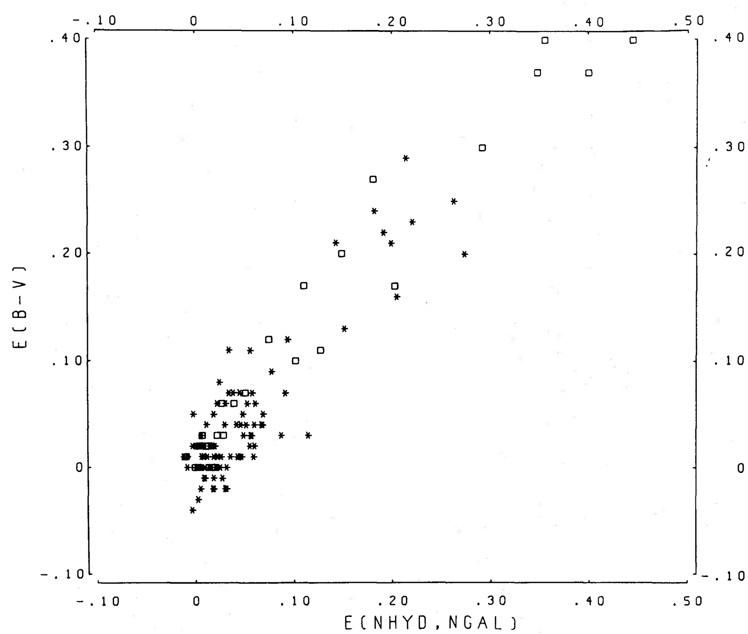

FIG. 6*b*

FIG. 6.—$E(B-V)$ from Table 1 versus $E(B-V)$, predicted from (*a*) eq. (4) and (*b*) eq. (6), for the globular clusters and RR Lyrae stars included in each fit, respectively (see text). Squares represent globular clusters; stars represent stars.

using the same weighting scheme, is 0.037 mag—again much larger than for equations (4) and (6), when one considers the fact that most of the points have small values of N_H so that they are not affected much by R. The better fit for equations (4) and (6) represents confirmation of the variable gas-to-dust ratio found in § VI*a*.

Objects having $\delta < -23°$ lie outside of the area covered by the SW counts. For these objects, application of equation (7) with the values derived from all the objects in Table 1 is recommended.

H I data for $\delta < -30°$ can be obtained from Heiles and Cleary (1978). Note that, as discussed in § VII*a*, the value of x_1 in equation (4) and z_1 in equation (7) depends on the detailed characteristics of the equipment used for making the 21 cm line observations. The value of x_1 given in Table 3 is probably representative of data taken with typical parabolic telescopes and probably applies to Heiles and Cleary's southern survey.

VII. RAMIFICATIONS FOR THE INTERSTELLAR MEDIUM

a) *The Zero Offset*

The significantly nonzero value of x_1 found in equation (4) (and the similar value found in eq. [6], as discussed in § VI*b*) implies that a nonzero amount of H I must exist before the extinction begins to increase with the H I column density. However, some, and possibly all, of this zero offset can be explained by an instrumental effect, the response of the radio telescope to stray radiation.

Telescopes at all wavelengths are responsive to stray light which is scattered or diffracted onto the detector from directions other than that where the telescope is pointed. Radio telescopes are particularly subject to this problem, for two reasons. First, the structural members of the telescope have dimensions comparable to a wavelength, which makes diffraction effects particularly severe. Second, it is impossible to build a feed which responds only to the radiation reflected from the surface of the telescope (Ruze 1976). The feed responds to radiation from other directions as well, and particularly serious is the "spillover" region just outside the rim of the reflector. We note that telescopes can be built which do not have such problems; a good example is the horn reflector antenna of the Bell Telephone Laboratories at Crawford Hill, Holmdel, New Jersey, which has been used for some 21 cm line work for which stray radiation was especially deleterious (see review by Heiles and Wrixon 1976), and was used for the first detection of the 3 K cosmic background radiation (Penzias and Wilson 1965). Feeds used with parabolic reflectors in radio astronomy typically have 10%–20% of their response coming from this stray radiation (Rusch 1976). The importance of this stray radiation was first realized by the Dutch observers (Raimond 1966) and has recently been reemphasized by Giovanelli *et al.* (1978) and by Kalberla (Mebold 1977).

For example, the error in the value of N_H corresponding to the value of x_1 in equation (4) is $-x_1/x_2 = 100$ (or 2.3×10^{20} cm^{-2}); this is 2–4 times larger than the contributions from stray radiation estimated by Kalberla (Mebold 1977) and those we infer from the material presented by Giovanelli *et al.* (1978). Unfortunately, the relevant characteristics of the feed system which was used for the Hat Creek 21 cm line surveys are not well known and cannot now be investigated because a different feed system has been substituted.

Although we have no *a priori* reason to expect the Hat Creek system to have been more sensitive to stray radiation than other paraboloidal radio telescopes, we cannot rule out this possibility. A conservative approach would perhaps assign all of the zero offset to this cause until further evidence were available. The required excess sensitivity to stray radiation relative to similar telescopes is large enough, however, to cast doubt on such an explanation. If the effect were real, it would imply the existence of high-latitude gas without any appreciable associated dust. New 21 cm line measurements with a telescope that has little response to stray radiation are needed to settle the question.

b) *The Variable Gas-to-Dust Ratio—Not Just a Result of* H II *or* H_2

Figures 4*b* and 5 show an extremely large variation in the gas-to-dust ratio. However, some of this variation probably arises from a separate dependence of log N_{gal} on csc $|b|$ (see § VI*a*). Thus the variation in the gas-to-dust ratio is smaller than that exhibited in these figures.

The reddening data discussed in § VI*b* show that the residual R is a reasonably good measurement of the gas-to-dust ratio. From the map of R in galactic coordinates (Fig. 9 in Heiles 1976), regions with $R < 0$ have $dE(B-V)/dN_H$ larger than usual; i.e., they have a deficiency of H I. Such regions include the dusty regions in Ophiuchus, Perseus, and Orion—the Gould Belt regions. The most likely cause of these negative values of R is the presence of H_2, which is not detected in the 21 cm line.

But this cannot be the whole explanation. There are regions having nonzero values of R in which no H_2 or H II is known, or expected, to exist. For example, an area bounded by $l \approx 20°$ to $40°$, $b \approx -10°$ to $-30°$ has $-6 < R < -2$. The H I column density in this area is not particularly high, ranging from $N_H = 200$ to $N_H = 700$ (with the higher values occurring only for $b > 15°$). In the center of this area $E(B-V)$, derived from equation (4), equals 0.17 mag. Although there are no stars for which H_2 column densities have been measured in this region, the correlations of Savage *et al.* (1977) imply that less than 25% of the hydrogen is in molecular form. The Hα intensity (Reynolds, Roesler, and Scherb 1974; Sivan 1974) is too weak to account for the "missing" gas in the form of H II.

The fact that $E(B-V)$ can be predicted to be negative can be thought of as being a result of the variable gas-to-dust ratio; but these negative values are, of course, dictated by our conclusion that there is little or no reddening in areas where $N_H = 100$. Since $E(B-V) < 0.00$ is unphysical, all such cases should be set equal to 0.00.

It is curious that Figure 4*b* implies that the gas-to-dust ratio, as measured by the parameter B in equation (1), is correlated with longitude irrespective of latitude. The larger ratio at low longitudes for both positive and negative latitudes, for example, seems to imply that the variability of this ratio is not simply a Gould Belt phenomenon. This should be studied further, preferably by correlating the 21 cm measurements with $E(B-V)$ data determined for specific objects lying well away from the galactic plane.

We conclude that the total gas-to-dust ratio, where total gas includes H I, H II, and H_2, is variable. The amount of variability is quite high. Values of R vary from about -6 to $+6$ in the extreme, corresponding to a range in $dE(B - V)/dN_H$ from 0.15×10^{-3} to 0.56×10^{-3}—a factor of 4. This is similar to the range of variation in total gas to dust found by Bohlin (1975), by Savage *et al.* (1977), and by Bohlin, Savage, and Drake (1977).

VIII. SUMMARY

When compared with galaxy counts and H I column densities, our reddening data do not exhibit a latitude dependence of the type found by Heiles (1976), which was apparently produced by subtle biases in the reddening data he used. We believe that our reddening data are free of such biases. Furthermore, our data are consistent with small reddening at the galactic poles, which is expected both from surveys of interstellar extinction using galactic (e.g., McClure and Crawford 1971) and extragalactic (e.g., Sandage 1973) objects, and from the minimal density of interstellar gas observed in the immediate vicinity of the Sun (e.g., Henry *et al.* 1976).

Galaxy counts should be a reliable indicator of extinction, decreasing in number in regions of higher obscuration. The quantity $[-d(\log N_{gal})/d(A)]$, usually denoted by γ, must be approximately 1.0 for consistency with the general accepted value of $\mathscr{R} = A_{pg}/E(B - V) = 4.0$.

The "histogram" method of analyzing galaxy counts shows that the galaxy count data are too noisy to allow determination of the slope of a csc law near the galactic poles. We conclude that all available data, both from photometry and from galaxy counts, are consistent with there being little or no reddening at the NGP; that there may be somewhat more reddening at the SGP; and that the reddening at the NGP and probably also at the SGP is very irregularly distributed.

The H I column density alone cannot accurately predict extinction because of variations in the gas-to-dust ratio. Furthermore, there is a zero offset in the relation between reddening and H I column density. This offset may be caused by instrumental effects in the radio measurements, although this is unlikely. The zero offset has caused extinctions previously derived from H I data to be too large in regions of small H I column density.

Reddening cannot be predicted accurately either from galaxy counts alone or from the H I data alone. It can be predicted accurately by use of these data together. They both are used to derive the gas-to-dust ratio, which apparently varies slowly with position and by up to a factor of 2 from the average. This ratio is then used with H I data to derive the reddening from either equation (4) or (6). Equations (4) and (6) give equivalent results for $|b| > 15°$ and/or $E(B - V) < 0.3$ mag. Thus, in these regimes, it is recommended that one determine R (= gas-to-dust-ratio correction) from the map of Heiles (1976, Fig. 9), obtain N_H from the map of Heiles (1975), and use equation (4) to determine $E(B - V)$. For $|b| = 15°$, or values of $E(B - V)$ anticipated to be greater than 0.3 mag (e.g., when $N_H \gtrsim 800$), equation (6) is the better predictor of reddening, since it does not contain a csc $|b|$ term. However, log N_{gal} is currently mapped only in SW in 4 deg^2 smoothed averages. To obtain 13 deg^2 averages, one must further smooth the SW map. For either equation (4) or (6), if $E(B - V)$ is predicted to less than 0.00, set $E(B - V) = 0.00$. Both methods appear to be accurate to 0.03 mag in $E(B - V)$ for all areas of the sky covered by the SW counts. For the southern part of the sky, with no galaxy counts available, use of equation (7) is necessary, with the knowledge that relatively large percentage errors can be made in the prediction of $E(B - V)$ owing to variations in the gas-to-dust ratio.

It is a pleasure to thank Drs. M. Cleary, E. Jenkins, U. Mebold, C. D. Shane, and S. M. Faber for helpful discussions. We also thank Dr. L. H. McDonald for providing his observational results before publication and for assistance in compiling the RR Lyrae reddening data. Finally, we sincerely thank Dr. A. E. Whitford, who not only materially contributed to the final form of this paper, especially § IV, but also acted as the catalyst for many of our ideas.

REFERENCES

Abt, H. A., and Golson, J. C. 1962, *Ap. J.*, **136**, 363.
Alcaino, G. 1975, *Astr. Ap. Suppl.*, **21**, 15.
Allen, R. W. 1976, *Astrophysical Quantities* (3d ed.; London: Athlone Press).
Bohlin, R. C. 1975, *Ap. J.*, **200**, 402.
Bohlin, R. C., Savage, B. D., and Drake, J. F. 1977, preprint.
Burstein, D. 1978*a*, in preparation.
———. 1978*b*, Ph.D. thesis, University of California, Santa Cruz.
Burstein, D., and Heiles, C. 1978, *Ap. Letters*, **19**, 67 (Paper I).
Burstein, D., and McDonald, L. H. 1975, *A.J.*, **80**, 17.
Cannon, R. D. 1974, *M.N.R.A.S.*, **167**, 551.
de Vaucouleurs, G., and Malik, G. M. 1969, *M.N.R.A.S.*, **142**, 387.
Epstein, I., and de Epstein, A. E. A. 1973, *A.J.*, **78**, 83.
Fejes, I., and Wesselius, P. R. 1973, *Astr. Ap.*, **24**, 1.
Giovanelli, R., Haynes, M. P., York, D. G., and Shull, J. M. 1978, *Ap. J.*, **219**, 60.
Groth, E. J., and Peebles, P. J. E. 1977, *Ap. J.*, **217**, 385.
Harris, W. E. 1975, *Ap. J. Suppl.*, **29**, 397.
———. 1976, *A.J.*, **81**, 1095.
Harris, W. E., and Racine, R. 1974, *J.R.A.S. Canada*, **68**, 263.
Harris, W. E., Racine, R., and de Roux, J. 1976, *Ap. J. Suppl.*, **31**, 13.
Harris, W. E., and van den Bergh, S. 1974, *A.J.*, **79**, 31.
Heiles, C. 1975, *Astr. Ap. Suppl.*, **20**, 37.
———. 1976, *Ap. J.*, **204**, 379.
Heiles, C., and Cleary, M. N. 1978, in preparation.
Heiles, C., and Jenkins, E. B. 1976, *Astr. Ap.*, **46**, 333.
Heiles, C., and Wrixon, G. T. 1976, in *Methods of Experimental Physics*, ed. M. L. Meeks (New York: Academic Press), p. 58.
Henry, P., Bowyer, S., Lampton, M., Paresce, F., and Cruddace, R. 1976, *Ap. J.*, **205**, 426.
Hilditch, R. W., Hill, G., and Barnes, J. V. 1977, *M.N.R.A.S.*, **176**, 175.
Holmberg, E. B. 1974, *Astr. Ap.*, **35**, 121.
Illingworth, G., and Illingworth, W. 1976, *Ap. J. Suppl.*, **30**, 227.
Jenkins, E. B., and Savage, B. D. 1974, *Ap. J.*, **187**, 243.
Klemola, A. 1977, private communication.

Knapp, G. R., and Kerr, F. J. 1974, *Astr. Ap.*, **35**, 361.
Lee, S.-W. 1977, *Astr. Ap. Suppl.*, **27**, 367.
McClure, R. D., and Crawford, D. L. 1971, *A.J.*, **76**, 31.
McDonald, L. H. 1977, Ph.D. thesis, University of California, Santa Cruz.
McGillivray, H. T. 1975, *M.N.R.A.S.*, **170**, 241.
Mebold, U. 1977, private communication.
Menzies, J. 1974, *M.N.R.A.S.*, **168**, 177.
Neckel, H. 1965, *Zs. f. Ap.*, **62**, 180.
Penzias, A. A., and Wilson, R. W. 1965, *Ap. J.*, **142**, 419.
Racine, R., and Harris, W. E. 1975, *Ap. J.*, **196**, 413.
Raimond, E. 1966, *Bull. Astr. Inst. Netherlands Suppl.*, **1**, 33.
Reynolds, R. J., Roesler, F. L., and Scherb, F. 1974, *Ap. J. (Letters)*, **192**, L53.
Roach, F. E., and Gordon, J. L. 1973, *The Light of the Night Sky* (Dordrecht: Reidel).
Rusch, W. V. T. 1976, in *Methods of Experimental Physics*, Vol. **12b**, ed. M. L. Meeks (New York: Academic Press), p. 64.
Ruze, J. 1976, in *Methods of Experimental Physics*, Vol. **12b**, ed. M. L. Meeks (New York: Academic Press), p. 29.
Sandage, A. 1973, *Ap. J.*, **183**, 711.
Savage, B. D., Bohlin, R. C., Drake, J. F., and Budich, W. 1977, *Ap. J.*, **216**, 291.
Seki, M. 1973, *Astr. Ap.*, **28**, 207.
Seldner, M., Siebers, B., Groth, E. J., and Peebles, P. J. E. 1977, *A.J.*, **82**, 249.
Shane, C. D., and Wirtanen, C. A. 1967, *Pub. Lick Obs.*, **22**, 1 (SW).
Sivan, J. P. 1974, *Astr. Ap. Suppl.*, **16**, 163.
Stebbins, J., Whitford, A. E., and Johnson, H. L. 1950, *Ap. J.*, **112**, 469.
Stetson, P. B., and Harris, W. E. 1977, *A.J.*, **82**, 954.
Sturch, C. 1966, *Ap. J.*, **143**, 774.
———. 1969, *A.J.*, **74**, 82.
Walker, M. F., Pike, C. D., and McGee, J. D. 1976, *M.N.R.A.S.*, **175**, 525.

DAVID BURSTEIN: Department of Terrestrial Magnetism, Carnegie Institution of Washington, 5241 Broad Branch Road, N.W., Washington, DC 20015

CARL HEILES: Department of Astronomy, University of California, Berkeley, CA 94720